Low-temperature combustion of CH_4 over CeO_2–MO_x solid solution ($M = Zr^{4+}$, La^{3+}, Ca^{2+}, or Mg^{2+}) promoted Pd/γ–Al_2O_3 catalysts

Lihua Xiao, Kunpeng Sun*, Yuxia Yang, and Xianlun Xu

State Key Laboratory for Oxo Synthesis and Selective Oxidation, Lanzhou Institute of Chemical Physics, Chinese Academy of Sciences, Lanzhou 730000, China

Received 4 December 2003; accepted 24 March 2004

The catalytic behavior of Pd (2 wt%) catalysts supported on γ-Al_2O_3 and promoted with $CeO_2 - MO_x$($M = Zr^{4+}$, La^{3+}, Ca^{2+}, or Mg^{2+}) solid solution was investigated for methane combustion. The results demonstrated that Pd/γ-$Al_2O_3CeO_2$ MO_x catalysts can be effective for the low-temperature catalytic combustion of methane and are comparable in activity to other conventional catalysts for this reaction. The XPS and XRD results indicated that an enhanced mobility of lattice oxygen induced by the perturbation of Ce–O lattice was responsible for an increased catalytic performance during oxidation reaction. The most active sites in the catalyst system involve contacts between Pd and the CeO_2–MO_x mixed oxide component. Meanwhile, pre-treatment conditions have significant effect on the catalytic activity in methane combustion.

KEY WORDS: methane; combustion; CeO2–MO_x solid solution; Pd/γ-Al_2O_3; XPS; XRD.

1. Introduction

The catalytic combustion of methane over either noble metals or transition metal oxides has been extensively studied during last decades in view of developing catalytic combustion applications. The main advantage of noble metal catalysts over metal oxides is definitely their superior specific activity, which makes them as best candidates for low-temperature combustion of hydrocarbons. The catalytic activities of Pd catalysts supported on various metal oxides in the complete oxidation of methane at low-temperature were investigated by Widjaja *et al.* [1]. Recently, mixed oxide supports SnO_2–MO_x (M = Al, Ce, Fe, Mn, Ni, and Zr) were also prepared and the catalytic activity of Pd supported on these supports was studied [2]. No further improvement of the activity could be obtained by the use of mixed oxide supports compared to commercial SnO_2. The catalytic activities of Pd/Al_2O_3 catalysts modified by metal oxide additives (Ni, Sn, Ag, Rh, Mn, Pt, Co, Fe, Cr, Ce, and Cu) were studied by Ishihara *et al.* [3]. Among these binary supports, NiO added Pd/Al_2O_3 catalysts exhibited the highest activity for complete methane oxidation. Recently, CeO_2 has been widely applied as an additive in automotive catalysts due to its enhanced oxygen storage capacity (OSC). Moreover, the formation of solid solution between CeO_2 and some foreign cations (such as Zr^{4+}, Y^{3+}, La^{3+}, Sc^{3+}, Mg^{2+}, and Ca^{2+}, which can be introduced into the CeO_2 lattice) will improve the physical properties of CeO_2 [4]. It has been suggested that ceria structural modifications mediated by zirconia and zirconia-stabilized defects in ceria are responsible for the special properties of $Ce_xZr_{1-x}O_2$ [5]. Indeed, the use of $Ce_xZr_{1-x}O_2$ as a promising support of noble metals for methane combustion [6], NO decomposition [7], and methanol decomposition [8] has shown a rapid increase in the last years.

In this work, the CeO_2–MO_x solid solution modified Pd/γ-Al_2O_3 catalysts were prepared and examined for low-temperature combustion of methane in view of finding more effective supports for methane combustion.

2. Experimental

2.1. Catalyst preparation

The supports CeO_2–MO_x–Al_2O_3 (containing 30 wt% CeO_2–MO_x with a Ce/M molar ratio = 4; for MO_x free support, e.g., CeO_2–Al_2O_3, the content of CeO_2 was 30 wt%) were prepared by a deposition–precipitation method. In short, an aqueous solution of 0.25 M Na_2CO_3 was added drop-wise to an aqueous mixture of $Ce(NO_3)_3$ and nitrate of M and γ–Al_2O_3 powder until the pH value reached 10 under vigorous stirring. The resulting suspension was aged for 3 h under stirring, and was then washed several times with distilled water. The precipitate was filtered, dried at 120 °C, and finally calcined in air at 600 °C for 6 h. Palladium was then deposited onto the resultant support in the same manner followed by drying and calcining at 550 °C in air for 3 h. In all case, a $PdCl_2$ solution was used as the metal precursor. The loadings of Pd in the catalysts were set to be 2.0 wt%.

*To whom correspondence should be addressed.

1011-372X/04/0600–0151/0 © 2004 Plenum Publishing Corporation

2.2. Catalytic activity test

The catalytic combustion of methane was carried out in a conventional fixed-bed flow micro-reactor at atmospheric pressure. Catalyst sample of 0.5 mL (20–30 mesh) was packed in a quartz tube, which was connected with a thermocouple centered in the catalyst bed. Prior to the catalytic activity test, catalyst samples were subjected to a further treatment in two ways: (i) catalysts were reduced in a H_2 flow (10% in Ar) at 400 °C for 1.0 h and then aged with a reaction gaseous mixture (1 vol% CH_4 in air) for 0.5 h at 300 °C; (ii) catalyst samples were aged with reaction gaseous mixture for 0.5 h at 300 °C without any other treatment. In all tests, a constant space velocity of 50,000 h^{-1} was maintained and the temperature of reactor was raised from 200 °C up to no methane could be detected with a heating rate of 5 °C min^{-1}. The conversion of CH_4 was analyzed by an on-line gas chromatogram equipped with a flame ionization detector (FID) and methanation oven for the detection of CH_4, CO, and CO_2. The overall activity of catalyst was presented by temperatures at which methane conversion reaches 10 (defined as light-off temperature), 50, 90, and 100%, as expressed by $T_{10,}$ T_{50}, T_{90}, and T_{100}, respectively.

2.3. Catalyst characterization

X-ray diffraction (XRD) data of catalysts were collected on a Rigaku Dmax-B diffractometer (CuK_α radiation, 50 kV, 60 mA). The BET surface areas of catalysts were calculated from the nitrogen adsorption isotherm at 77 K measured in a Micromeritics ASAP2010 apparatus. The average palladium particles size was estimated from CO chemisorption using a conventional glass volumetric apparatus. Prior to the measurements, 1.0 g of the sample placed in a glass tube was reduced in hydrogen at 40 kPa and 400 °C for 0.5 h, evacuated at 400 °C for 1 h, and then cooled to room temperature in a vacuum. Measurements were carried out at room temperature and low pressure (<1.3 kPa) until CO adsorption reached apparent equilibrium. The dispersion and particle size of palladium were calculated by assuming a stoichiometric adsorption of CO/Pd = 1. XPS were acquired on a PHI 550 photoelectron spectrometer equipped with an MgK_α ($hv = 1253.6$ eV). Measurements were performed at room temperature and at normal emission angles. Prior to *in situ* XPS measurement, typical treatment and reaction procedures as above were precisely simulated in a dedicated "preparation chamber" which was connected to XPS spectrometer as follows: (i) catalyst samples were treated as stated in catalytic tests; (ii) catalytic combustion reaction was simulated at T_{100} over corresponding catalyst, respectively; (iii) the reaction gas was swept out by N_2 (99.99%) in order to keep real states of catalysts. The reactor was then outgassed and cooled to room temperature. And then, the "preparation chamber" was transferred to the analysis chamber. The residual pressure in the ion-pumped analysis chamber was maintained below 3.0×10^{-9} mbar (1 mbar = 101.33 Pa) during data acquisition. Binding energies were calculated with respect to C(1s) at 285.00 eV. Binding energies were measured with a precision of 0.2 eV.

3. Results and discussion

Catalytic activities for methane combustion over various supported Pd catalysts are summarized in table 1. In all cases, no reaction products except carbon dioxide and water were detected. Clearly, it can be seen that the catalytic activities were observed to depend on the supports and also the pre-treatment conditions. Let us discuss the data obtained over catalysts aged in reaction gaseous mixture first. The oxidation of methane over Pd/Al_2O_3 catalyst started at about 250 °C followed by a steady increase in conversion up to 100% at 423 °C. A slight increase in catalytic activity was observed when ceria was added to Pd/Al_2O_3. This fact was in good agreement with the results reported previously [9,10]. However, the catalytic activity was significantly enhanced by the presence of foreign cations incorporated in the Al_2O_3–CeO_2 support. In particular, the $Pd/Al_2O_3CeO_2La_2O_3$ catalyst exhibited light-off temperature shifted by more than 20 °C toward lower temperatures compared to Pd/Al_2O_3 catalyst. Surprisingly, pre-reduction of catalysts prior to being aged enhanced the catalytic activities, for Pd/Al_2O_3 and $Pd/Al_2O_3CeO_2$ weakly, for the other catalysts strongly. $Pd/Al_2O_3CeO_2CaO$ catalyst followed by $Pd/Al_2O_3CeO_2La_2O_3$, exhibited the lowest light-off temperature.

XRD patterns of catalysts are shown in Figure 1. All the catalysts were calcined at 600 °C for 6 h without any further pre-treatment. No legible reflections of PdO and MO_x were detected. Despite the fact that, the amount of Al was higher than that of Ce in catalysts, the intensity corresponding to the γ–Al_2O_3 was much smaller than that of CeO_2. Therefore, the CeO_2–MO_x mixed oxides are most likely present in a highly dispersed form on the surface of the γ-Al_2O_3 particles. The accurate evaluation

Table 1
Catalytic activities in methane combustion catalyzed over supported palladium catalysts

Catalyst	Aged with 1%CH_4 in air				Pre-reduced with H_2 before aged			
	T_{10}	T_{50}	T_{90}	T_{100}	T_{10}	T_{50}	T_{90}	T_{100}
Pd/Al_2O_3	307	349	398	423	305	350	389	416
$Pd/Al_2O_3CeO_2$	305	346	393	417	299	343	378	409
$Pd/Al_2O_3CeO_2MgO$	303	345	383	409	259	314	360	386
$Pd/Al_2O_3CeO_2ZrO_2$	297	344	381	403	273	324	360	377
$Pd/Al_2O_3CeO_2CaO$	296	340	374	386	249	310	349	367
$Pd/Al_2O_3CeO_2La_2O_3$	282	318	347	361	254	299	329	340

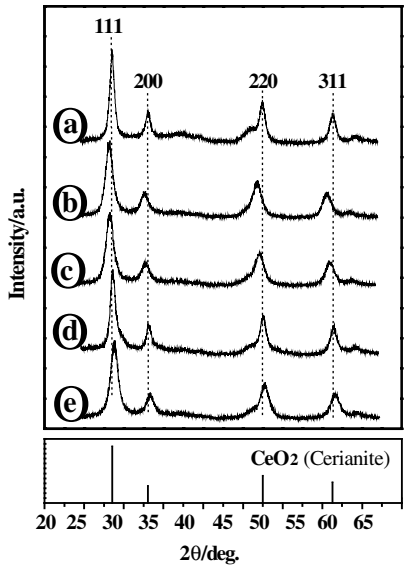

Figure 1. The XRD patterns of (a) $Pd/Al_2O_3CeO_2$; (b) Pd/Al_2O_3-$CeO_2La_2O_3$; (c) $Pd/Al_2O_3CeO_2CaO$; (d) $Pd/Al_2O_3CeO_2ZrO_2$ and (e) $Pd/Al_2O_3CeO_2MgO$.

of the position of the main reflections of CeO_2 corresponding to the (111), (200), (220), and (311) crystallographic planes in $Pd/Al_2O_3CeO_2La_2O_3$ and $Pd/Al_2O_3CeO_2CaO$ catalysts showed a 2θ shift towards lower angles in the range of 0.10°–0.50° with respect to the positions of the same peaks in $Pd/Al_2O_3CeO_2$ catalyst. For $Pd/Al_2O_3CeO_2ZrO_2$ and $Pd/Al_2O_3CeO_2MgO$ catalysts, the 2θ shifted toward higher angles in the range of 0.09°–0.12°. This is probably due to the formation of CeO_2–MO_x solid solution caused by dissolution of M ions into CeO_2 lattice. Knowledge of the lattice parameters can provide information on the compositions or an analysis of the defect structure in the CeO_2–MO_x solid solution. Therefore, the precise lattice parameters of CeO_2 in the catalyst system were determined and tabulated in table 2, together with BET surface areas and the crystallite sizes of CeO_2. These lattice parameters give important information when compared with pure CeO_2 cell that has a generally

Table 2
Main physical properties from XRD, BET, and CO chemisorption

Sample	Lattice parameter of CeO_2 cell (Å)	CeO_2 average particle size (nm)[a]	S_{BET} (m^2/g)	Pd dispersion[b]	Pd particle size (nm)[b]
PdA	–	–	193	0.26	5.1
PdAC	5.4137	12.0	170	0.38	4.6
PdACM	5.4054	7.3	148	0.53	3.6
PdACZ	5.4072	8.9	144	0.56	3.4
PdACC	5.4156	8.7	154	0.55	3.4
PdACL	5.4503	7.6	148	0.67	2.9

[a]Crystallite sizes of CeO_2 were estimated using Scherrer's equation.
[b]Pd dispersion and particle sizes were measured by CO chemisorption.

accepted value of 0.541134 nm. The $Pd/Al_2O_3CeO_2MgO$ and $Pd/Al_2O_3CeO_2ZrO_2$ show negative expansions as expected since Zr^{4+} (0.84 Å) and Mg^{2+} (0.89 Å) have an ionic radius that is just below Ce^{4+} (0.97 Å). However, The $Pd/Al_2O_3CeO_2CaO$ and $Pd/Al_2O_3CeO_2La_2O_3$ samples exhibit obvious expansion of the lattice parameters as expected since Ca^{2+} (1.15 Å) and La^{3+} (1.19 Å) have larger ionic sizes than Ce^{4+}. The highest Pd dispersion was achieved on $Pd/Al_2O_3CeO_2La_2O_3$. The average palladium particle size increased in the sequence $Pd/Al_2O_3CeO_2La_2O_3 < Pd/Al_2O_3CeO_2CaO \approx Pd/Al_2O_3$ $CeO_2ZrO_2 < Pd/Al_2O_3CeO_2MgO < Pd/Al_2O_3CeO_2 <$ Pd/Al_2O_3. Since BET surface areas were similar for all the catalysts, expect for Pd/Al_2O_3 and $Pd/Al_2O_3CeO_2$, the structure of cerium oxide and the type of support might contribute to the distribution of the palladium particles. It can be pointed out that the addition of MO_x is favorable for the dispersion of palladium on Al_2O_3, which partly contributes to the higher catalytic activities of $Pd/Al_2O_3CeO_2MO_x$.

Table 3 presents some data determined from XPS characterization. Recent XPS studies [11,12] of PdO show that the binding energy of $Pd3d_{5/2}$ in PdO is at 336.8 eV, the BE values for $Pd3d_{5/2}$ of working catalysts except for Pd/Al_2O_3 in this study, are significantly higher than that of PdO. This result implies that Pd^{2+} ions in the system are much more cationic than PdO. It is necessary to remind some possible reasons for the formation of such cationic PdO species in order to gain some insights into the beneficial effect of promoters. Usually, the species could be attributed to a highly dispersed and deficiently coordinated (ionic) Pd^{2+} in intimate contact with the support (e.g., SMSI effect). The formation of CeO_2–MO_x solid solution strongly perturbs the symmetry of Ce–O and/or M-O bond. The perturbation of Ce–O and/or M-O bond, which leads to highly disordered oxygen in the lattice, promotes the oxygen transfer from the bulk to the support surface and from the support to the Pd particles. As a result, CeO_{2-x} defects are formed in the form of Ce^{3+}, which in the Kröger—Vink notation is written as $Cé_{Ce}$ as the Ce^{3+} has on negative charge compared to the normal lattice:

$$O_O + 2Ce_{Ce} = 1/2O_2(gas) + V_O^{\cdot\cdot} + 2Ce'_{Ce} \qquad (1)$$

where O_O is the lattice oxygen in the CeO_2, Ce_{Ce} is the cerium in the lattice of CeO_2, $V_O^{\cdot\cdot}$ is the oxygen vacancy [13]. Thereby, the increase in oxygen mobility can not only maintain the Pd in a more cationic Pd^{2+} state [8] but also facilitate methane oxidation reaction. In the O1s spectra (not shown), a contribution at the low BE value side (centered at 529.5 eV, named O_{II}), besides the main peak (named O_I) at about 531.2–531.5 eV, was observed on all the samples except for Pd/Al_2O_3. The major peak component, e.g., O_I, is the characteristic of Al–O group, component O_{II} belongs most likely to lattice oxygen on the surface of CeO_2–MO_x solid solution [14,15]. According to area of peaks, $[O_{II}/O_I]$

Table 3
Summarized data for supported catalysts determined from XPS analysis

Catalyst	BE value of $Pd3d_{5/2}$ (ev)	Surface component (at%)			$\frac{[OII]}{[OI]}$
		Pd	Ce	Al	
$PdAl_2O_3$	336.7 (336.8)	0.18 (0.17)	–	26.1 (26.9)	0 (0)
$Pd/Al_2O_3CeO_2$	337.1 (337.2)	0.71 (0.54)	33.2 (14.4)	12.8 (20.1)	0.32 (0.35)
$Pd/Al_2O_3CeO_2MgO$	337.3 (337.5)	1.2 (1.1)	25.0 (25.4)	12.1 (13.9)	0.44 (0.55)
$Pd/Al_2O_3CeO_2ZrO_2$	337.4 (337.6)	0.69 (0.43)	23.6 (40.7)	11.7 (14.7)	0.44 (0.57)
$Pd/Al_2O_3CeO_2CaO$	337.5 (337.6)	0.64 (0.87)	47.4 (24.8)	8.8 (12.7)	0.46 (0.61)
$PdAl_2O_3CeO_2La_2O_3$	337.5 (337.6)	1.1 (1.2)	22.1 (20.6)	13.2 (12.9)	0.49 (0.67)

Note. Values corresponding to aged and pre-reduced/aged catalysts are listed outside and inside parentheses, respectively.

ratio was obtained as shown in table 3. Comparing the $[O_{II}/O_I]$ ratio of each modified Pd/Al_2O_3 catalyst, one can find that the enrichment of lattice oxygen was formed on pre-reduced/aged samples compared to that on only aged samples. More lattice oxygen produced by the perturbation of Ce–O and/or M–O was indicated as responsible for an increased catalytic performance during combustion reaction over pre-reduced/aged samples. In fact, reports about the correlation between the activity in methane oxidation and the lattice oxygen have been published since the publication of the original work by Mars and van Krevelen [16]. Previously, Haneda *et al.* [17] proposed that methane oxidation over CeO_{2-x}/Al_2O_3 proceeds through the dissociation and diffusion of adsorbed oxygen into the surface vicinity of CeO_{2-x} crystallites, and then the reaction occurred between the lattice oxygen formed and methane. Methane oxidation over $Pd/Al_2O_3CeO_2MO_x$ catalysts is presumed to proceed in a similar reaction mechanism, but the presence of Pd enhances the methane oxidation even at low temperature. Because of the high oxygen mobility on CeO_2–MO_x surface, vacancies created near the palladium particles are rapidly refilled by migration of oxygen from the bulk of supports and gas phase, and the oxygen distribution on the surface is equilibrated. By contrast, the oxygen vacancies on the alumina-supported catalyst whose oxygen mobility is lower are refilled mainly from the gas phase [18]. Namely, the oxygen from the support also participates in the methane combustion reaction over $Pd/Al_2O_3CeO_2MO_x$. It was proposed that the lattice vacancies in CeO_{2-x} store the spillover oxygen from Pd to maintain the active palladium, and the oxygen generated from CeO_{2-x} migrates onto Pd, on which methane could be dissociated, by the reverse spillover [17]. Consequently, it is plausible to suggest that most active sites in the CeO_2–MO_x modified Pd/γ-Al_2O_3 catalysts involve contacts between Pd and the CeO_2–MO_x mixed oxide component.

The quantitative XPS analysis showed that catalysts with different supports under different pre-treatment conditions exhibited various surface concentration of Pd, Ce, and Al (see ''surface component'' in table 3). Notably, $Pd/Al_2O_3CeO_2CaO$ showed higher catalytic activity than $Pd/Al_2O_3CeO_2MgO$ in spite of the lower surface concentration of Pd on surface (0.64 at%) compared to $Pd/Al_2O_3CeO_2MgO$ (1.2 at %). The fact indicated that no simple correlation could be established between the catalytic activity and the Pd concentration on catalyst surface.

Although no attempt was made to distinguish exact nature of local structure on catalyst surface in the present study, the difference either in the particle or in morphology can be expected on the catalyst surface due to different pre-treatment conditions. For Voogt *et al.* [19], who investigated the oxidation of Palladium model catalysts by XPS analysis, a new oxide layer at oxide–metal interface was formed through the lattice reconstruction. For Datye *et al.* [20], a similar increase in the size of Pd crystallites accompanied by an increase in methane oxidation activity as these particles restructured to expose low–index surface planes was observed.

4. Conclusions

The main interesting conclusion to this study is that CeO_2–MO_x (M = Zr^{4+}, La^{3+}, Ca^{2+}, or Mg^{2+}) solid solution modified Pd/γ-Al_2O_3 catalysts can be effective for the catalytic combustion of methane and are comparable in activity to other conventional catalysts for this reaction. The oxygen mobility of the supports appears of crucial importance for the low-temperature catalytic combustion of methane. The most active sites in the catalyst system involve contacts between Pd and the CeO_2–MO_x mixed oxide component. Meanwhile, pre-treatment conditions have significant effect on the catalytic activity in methane combustion. In the end, we have to stress that there seems to be a reasonable explanation for the promoting effect of CeO_2–MO_x catalytic activity of Pd/Al_2O_3 in methane oxidation at this stage, while a variety of experimental approaches are still needed to provide corroborating and conclusive materials to fully understand the exact promoting effect in a further work.

References

[1] H. Widjaja, K. Sekizawa and K. Eguchi, Chem. Lett. (1998) 481.
[2] H. Widjaja, K. Sekizawa and K. Eguchi, Bull. Chem. Soc. Jpn. 72 (1999) 313.
[3] T. Ishihara, H. Shigematsu, Y. Abe and Y. Takita, Chem. Lett. (1993) 407.
[4] M. Pijolat, M. Prin and M. Soustelle, J. Chem. Soc. Faraday Trans. 91 (1995) 3941.
[5] J.A. Rodriguez, Catal. Today 85 (2003) 177.
[6] C. Bozo, N. Guilhaume and J.M. Herrmann, J. Catal. 203 (2003) 393.
[7] G.R. Rao, P. Fornasiero, R.D. Monte and J. Kaspar, J. Catal. 162 (1996) 1.
[8] Y. Liu, T. Hayakawa, T. Ishii and M. Kumagai, Appl. Catal. A 210 (2001) 301.
[9] G. Groppi, C. Critiani, L. Lietti, C. Ramella and M. Valentini, Catal. Today 50 (1999) 399.
[10] Y. Deng, T.G. Nevell, Catal. Today 47 (1999) 279.
[11] T. Pillo, R. Zimmermann and P. Steiner, J. Phys.: Condens. Matter 9 (1997) 3987.
[12] M. Burn, A. Berthet and J.C. Bertolini, J. Electron Spectrosc. Relat. Phenom. 104 (1999) 55.
[13] M. Mogensen, N.M. Sammes and G.A. Tompsett, Solid State Ionics 129 (2000) 63.
[14] S. Hamoudi, F. Larachi, A. Adnot and A. Sayari, J. Catal. 185 (1999) 333.
[15] C.D. Wagner, D.A. Zatko and R.H. Raymond, Anal. Chem. 52 (1980) 1445.
[16] P. Mars and D.W. van Krevelen, Chem. Eng. Sci. Suppl. 3 (1954) 41.
[17] M. Haneda, T. Mizushima and N. Kakuta, J. Chem. Soc. Faraday Trans. 91 (1995) 4459.
[18] D. Ciuparu, F.B. Verduraz and L. Pfefferle, J. Phys. B 106 (2002) 3434.
[19] E. H. Voogt, A.J.M. Mens, O.L.J. Gijzeman and J.W. Geus, Catal. Today 47 (1999) 321.
[20] A.K. Datye, J. Bravo, T.R. Nelson and L.D. Pfefferle, Appl. Catal. A 198 (2000) 179.